

## NONTHERMAL PROPERTIES OF SUPERNOVA REMNANT G1.9+0.3

L.T. KSENOFONTOV<sup>1</sup>, H.J. VÖLK<sup>2</sup>, AND E.G. BEREZHKO<sup>1</sup>*Draft version April 16, 2010*

## ABSTRACT

The properties of the – presumably – youngest Galactic supernova remnant (SNR) G1.9+0.3 are investigated within the framework of nonlinear kinetic theory of cosmic ray acceleration in SNRs. The observed angular size and expansion speed as well as the radio and X-ray emission measurements are used to determine relevant physical parameters of this SNR. Under the assumption that SNR G1.9+0.3 is the result of a Type Ia supernova near the Galactic center (at the distance  $d = 8.5$  kpc) the nonthermal properties are calculated. In particular, the expected TeV gamma-ray spectral energy density is predicted to be as low as  $\epsilon_\gamma F_\gamma \approx 5 \times 10^{-15}$  erg cm<sup>-2</sup> s<sup>-1</sup>, strongly dependent ( $F_\gamma \propto d^{-11}$ ) upon the source distance  $d$ .

*Subject headings:* acceleration of particles — ISM: individual (G1.9+0.3) — supernova remnants — X-rays: individual (G1.9+0.3) — gamma rays: observations

## 1. INTRODUCTION

G1.9+0.3 has been known as a potentially young shell type Galactic supernova remnant (SNR) of very small angular size (Green & Gull 1984). Recently, the interest in this SNR was revived by Reynolds et al. (2008, 2009) who analyzed the expansion rate of the object and deduced an age  $t_{\text{SN}}$  of about 100 yr, which makes it the youngest known SNR in the Galaxy. Although the expansion rate was derived by a comparison of radio observations in 1985 and *Chandra* observations in 2007, this rate has been confirmed very soon thereafter by independent radio observations (Green et al. 2008; Murphy et al. 2008).

According to Reynolds et al. (2008), the line-free X-ray emission has a pure synchrotron origin which clearly indicates that effective particle acceleration takes place, at least for electrons. There are also arguments, like the bilateral symmetry of the X-ray synchrotron emission suggesting a roughly uniform ambient magnetic field, that favor a type Ia origin for G1.9+0.3. Finally, the distance estimate  $d = 8.5$  kpc is based on an analysis of the absorption toward G1.9+0.3.

During the survey of the inner Galaxy by H.E.S.S. in very high energy  $\gamma$ -rays, no emission was reported from the direction to G1.9+0.3 (Aharonian et al. 2006). Therefore, one can derive an upper limit at the level of 2% of the Crab flux above 200 GeV.

For the purpose of a more general study of such an unusual object regarding its nonthermal properties, it is of interest to describe it by a kinetic theory of cosmic ray (CR) acceleration in SNRs, coupled with the gas dynamics of the thermal plasma, as given by Berezhko et al. (1996) and Berezhko & Völk (1997). This model assumes spherical symmetry, although the assumption is later relaxed. Similar models on almost the same physical basis have recently been developed by two other groups (Kang & Jones 2006;

Zirakashvili & Ptuskin 2009), whose calculations very well confirm these earlier results.

The kinetic description allows a corresponding analysis of the nonthermal evolution of an SNR at a very early phase. This assumes that the plasma physics underlying especially the temporal dependence of the magnetic field amplification process can be extrapolated to such an early evolutionary phase, where the dynamical behavior of the ejecta plays an essential role. Such a study is reported here. It is combined with a discussion about the influence of the assumption of a smaller distance on the TeV  $\gamma$ -ray flux.

## 2. MODEL

Following Reynolds et al. (2008) it is assumed that G1.9+0.3 is a Type Ia supernova (Type Ia SN) which expands into a uniform interstellar medium (ISM). Specifically, the object is assumed to eject a Chandrasekhar mass  $M_{\text{ej}} = 1.4M_\odot$  with a total hydrodynamic explosion energy  $E_{\text{SN}} = 10^{51}$  erg. During an initial period, the ejecta material has a broad distribution in velocity  $v$ . The fastest part of these ejecta is described by a power law  $dM_{\text{ej}}/dv \propto v^{2-k}$  with  $k = 7$  (e.g., Chevalier 1982).

The ISM mass density  $\rho_0 = 1.4m_p N_H$ , which is usually characterized by the hydrogen number density  $N_H$ , is an important parameter which strongly influences the expected SNR dynamics and nonthermal emission; here  $m_p$  denotes the proton mass.

Following Reynolds et al. (2008) also a distance  $d = 8.5$  kpc is adopted for the main part of the paper. The observed shock size  $R_s = 2$  pc and shock speed  $V_s = 14,000$  km s<sup>-1</sup> are then used to determine the SNR age  $t_{\text{SN}}$  and the ISM number density  $N_H$  for the given source distance  $d$ .

As reviewed earlier (Völk 2004; Berezhko 2005, 2008) and elaborated most recently in detail in Berezhko et al. (2009), the key parameters of the theoretical model (proton injection flux density, given by a constant injection parameter  $\eta \ll 1$  times the thermal particle flux density into the shock, electron-proton ratio below the synchrotron cooling range, later denoted as  $K_{\text{ep}}$ , and magnetic field amplification) can be estimated in a semi-empirical way from a fit of the theoretical solution to

Electronic address: ksenofon@ikfia.ysn.ru

<sup>1</sup> Yu.G. Shafer Institute of Cosmophysical Research and Aeronomy, 31 Lenin Ave., 677980 Yakutsk, Russia<sup>2</sup> Max Planck Institut für Kernphysik, Postfach 103980, D-69029 Heidelberg, Germany

the observed synchrotron emission spectrum if the characteristics of the initial explosion and the relevant astronomical parameters are known. For this purpose, the nonlinear aspects of the kinetic description are required.

Of the above-mentioned processes, the magnetic field amplification (Bell 2004) is the least well understood. It is connected with the strong nonlinear excitation of magnetic field fluctuations in the shock precursor by the accelerating energetic particles (McKenzie & Völk 1982; Lucek & Bell 2000; Bell & Lucek 2001; Bell 2004). Therefore, it is assumed here that these fluctuations lead to Bohm diffusion of the energetic particles in this amplified field. Such a bootstrap mechanism can be approximately justified by the results of recent particle simulations (Reville et al. 2008). In addition, the amplification process is strongly dissipative, as shown by hydromagnetic and kinetic simulations (Bell 2004; Zirakashvili et al. 2008; Reville et al. 2008; Niemiec et al. 2008; Riquelme & Spitkovsky 2009; Ohira et al. 2009). Therefore, it must be accompanied by strong gas heating within the precursor region  $r > R_s$  due to wave dissipation, adopted in the present model in the form  $(\partial e_g / \partial t)_{\text{diss}} = -\alpha_H c_A \partial P_c / \partial r$  with  $\alpha_H = 1$  (Berezhko et al. 1996; Berezhko & Völk 1997), where  $e_g$  is the gas thermal energy density,  $P_c$  denotes the energetic particle pressure, and where, in a second bootstrap mechanism,  $c_A = B(4\pi\rho)^{-1/2}$  is the Alfvén velocity in the amplified field  $B$  (see below). The value  $\alpha_H = 1$  corresponds to the assumption that the Alfvén wave field excited within the precursor reaches amplitudes which are very much smaller than the maximal amplitudes which could be reached if the whole work  $-c_A \partial P_c / \partial r$  done by CRs went into wave excitation. In such a case, this work goes almost completely into gas heating due to the wave damping. The gas thermal pressure just ahead of subshock is in this case considerably larger than the pressure of the magnetic field (Berezhko 2008). Therefore, the subshock can be treated approximately as a pure gas shock. This approximation will later be re-examined through the approximate inclusion of the amplified field and its associated turbulent gas motions in the subshock dynamics.

The magnitude of field amplification in all young SNRs is such that a non-negligible fraction of the shock energy  $\rho_0 V_s^2$  is converted into magnetic field energy (e.g. Berezhko 2008). In fact, a time dependent, amplified upstream magnetic field strength

$$B_0(t) = B_0(t_{\text{SN}})[V_s(t)/V_s(t_{\text{SN}})]^\delta \quad (1)$$

is used here, where the theory parameter  $B_0(t_{\text{SN}})$  is the rms field strength at the present epoch  $t_{\text{SN}}$  and is estimated by a comparison of the theoretically calculated synchrotron spectrum with the observed one (see below). Such a form of the time dependence of the amplified magnetic field with  $\delta \approx 1$  is consistent with the interior field strengths estimated from observational results for a number of young SNRs (e.g. Völk et al. 2005). (Since Bell (2004) even estimated a dependence  $B_0(t) \propto V_s^{3/2}(t)$  for the field amplification due to the nonresonant streaming instability alone, also the case of  $\delta = 3/2$  will be examined here. The radial dependence of the rms. magnetic field strength  $B(r, t)$  in the shock precursor is then modeled by  $B(r, t) = B_0(t)\rho(r, t)/\rho_0$ , where  $\rho_0$  is the far upstream (interstellar) density. In the overall con-

servation relations for momentum and energy of the system, the magnetic field strength in the upstream ISM is  $B_{\text{ISM}} < B_0$ . Thus,  $B_0/B_{\text{ISM}}$  is the field amplification factor by the accelerating energetic particles alone. An analysis performed for a number of young SNRs shows (e.g., Berezhko 2008) that the field strength  $B_0$ , required to fit the observed synchrotron spectrum, is well within the range expected from theoretical estimates (e.g., Bell 2004; Pelletier et al. 2006).

The observed X-ray morphology of SNR G1.9+0.3 agrees with the theoretical expectations regarding the morphology of ion injection and the corresponding morphology of magnetic field amplification for a Type Ia SN (Völk et al. 2003). It is therefore consistent with a correction for the spherically symmetric solution by a renormalization factor  $f_{\text{re}} \approx 0.2$  of the energy density of nuclear particles, like in the case of SN 1006 (Berezhko et al. 2009). In this case, the electron-proton ratio  $K_{\text{ep}}$ , calculated under the assumption of spherical symmetry, should be increased by a factor  $1/f_{\text{re}}$ .

### 3. RESULTS

The calculated evolution of the gas dynamical variables of G1.9+0.3 is shown in Figure 1. The observed shock radius  $R_s$  and shock speed  $V_s$  are fitted at the age  $t_{\text{SN}} = 80$  yr and for an ISM hydrogen number density  $N_{\text{H}} = 0.018 \text{ cm}^{-3}$  (Figure 1a). Since the remnant is in the free expansion phase, it is approximately consistent with an analytical self-similar solution  $R_s \propto t^{4/7}$  (Chevalier 1982). Note that an explosion model with an exponential ejecta velocity profile gives slightly larger values of the age,  $t_{\text{SN}} = 100$  yr, and of the ISM density, corresponding to a hydrogen number density of about  $N_{\text{H}} \approx 0.03 \text{ cm}^{-3}$ , for the same assumed distance of  $d = 8.5$  kpc (Reynolds et al. 2008).

The calculated radius  $R_c$  of the contact discontinuity (CD) and the CD speed  $V_c$  are also shown in Figure 1(a). One can see that the ratio  $R_c/R_s$  is rather small. At the current epoch  $R_c/R_s \approx 0.9$ .

To obtain a good fit for the observed synchrotron spectrum (see below) first of all a proton injection rate  $\eta = 10^{-3}$  is required. It leads to a nonlinear modification of the shock which, at the current age of  $t = 80$  yr, has a total compression ratio  $\sigma \approx 4.6$  and a subshock compression ratio  $\sigma_s \approx 3.6$  (Figure 1(b)). In addition, an electron-proton ratio  $K_{\text{ep}} \approx 5 \times 10^{-3}$  and an upstream amplified magnetic field strength at the current epoch  $B_0(t_{\text{SN}}) \approx 100 \text{ } \mu\text{G}$  are required. This implies a downstream magnetic field strength of  $B_d \approx 460 \text{ } \mu\text{G}$ .

All the above quantities are almost the same for the two different time dependences of the magnetic field  $B_0(t)$  within the evolutionary period  $t = t_{\text{SN}} \pm 100$  yr. The only difference between these cases is a slightly more rapid increase of the shock modification (characterized by the shock compression ratio  $\sigma(t)$ ) in the case  $\delta = 3/2$  compared with the case  $\delta = 1$  due to the increase of the Alfvénic Mach number  $M_A \propto V_s/B_0 \propto V_s^{1-\delta} \propto t^{3(\delta-1)/7}$ .

To explain these results it is noted that, as in other, similar cases of strong, modified shocks, the existing measurements permit an estimate of the three parameters of the theoretical model. This takes into account the following influence of the parameters on the synchrotron spectrum. (1) Since the high-energy electrons undergo strong synchrotron losses and, since during the

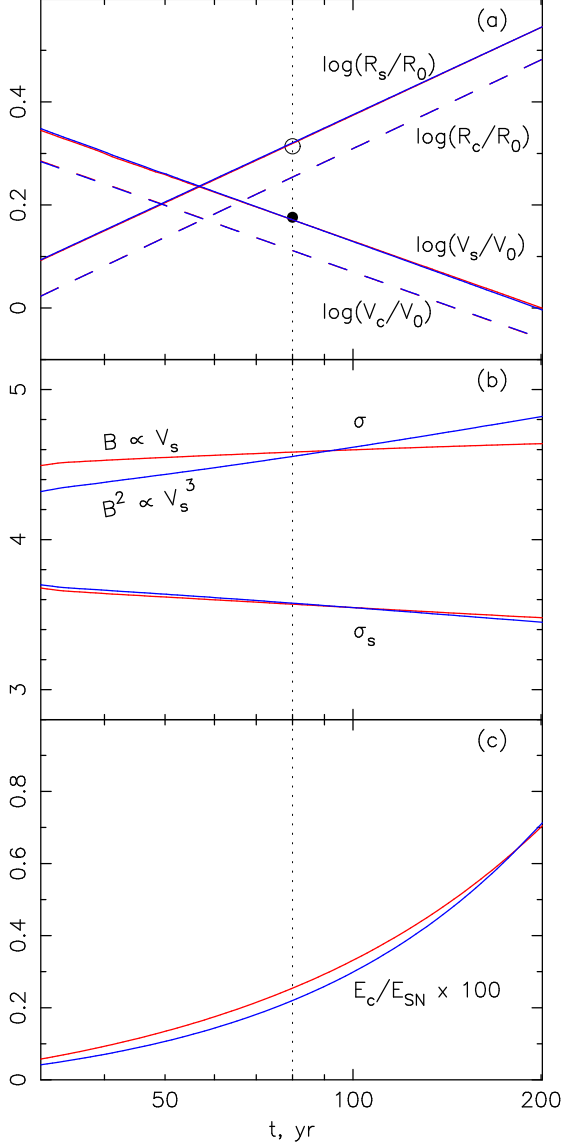


FIG. 1.— Shock (CD, (dashed lines)) radii  $R_s$  ( $R_c$ ) and shock (CD, (dashed lines)) speeds  $V_s$  ( $V_c$ ) in units of  $R_0 = 1$  pc and  $V_0 = 10^4$  km s $^{-1}$  (a), total shock  $\sigma$  and thermal subshock  $\sigma_s$  compression ratios (b), and total energy contents of accelerated CRs,  $E_c$  (c), as functions of time in years. The red colored curves imply an amplified magnetic field strength  $B \propto V_s(t)$ , whereas the blue colored curves correspond to  $B \propto V_s^{3/2}(t)$ , cf. Equation (1); the difference between these two cases is not distinguishable in Figure 1(a). The dotted vertical line marks the current epoch,  $t_{\text{SN}} = 80$  yr. The observed mean size (*open circle*) and speed (*filled circle*) of the shock, as determined by X-ray measurements (Reynolds et al. 2008), are shown as well.

acceleration process they dominate the nonthermal electron pressure  $P_e^e$ , the flux of X-ray synchrotron emission which they produce  $\nu S_\nu$  is approximately proportional to the total energy flux of nonthermal electrons  $F_e \propto P_e^e V_s R_s^2 \propto K_{\text{ep}} P_c V_s R_s^2$ , and is only weakly sensitive to the magnetic field strength  $B_0$ . The spectrum of high-energy protons  $N(p)$ , which give the main contribution to the total CR pressure  $P_c \sim \rho V_s^2$ , is only weakly sensitive to the injection parameter  $\eta$  in the case of a modified shock. Therefore, the fit of the *observed X-ray flux* mainly determines the value  $K_{\text{ep}}$  of the electron:proton ratio. The spectrum of accelerated electrons is calculated in absolute numbers. It is expressed in terms of

$K_{\text{ep}}$ , due to the presumably dominant dynamical role of protons. (2) Values  $\alpha > 0.5$  of the radio spectral index  $\alpha = -d \ln S_\nu / d \ln \nu$ , as observed in young SNRs, require a modified shock with  $\sigma_s < 4 < \sigma$  (This also implies a curved electron spectrum that hardens toward high frequencies). The value of  $\alpha$  is mainly determined by the subshock compression ratio  $\sigma_s$ , which in turn is determined mainly by the proton injection rate  $\eta$ . Therefore the fit of the *measured spectral shape* of the radio synchrotron emission gives mainly the required value of the injection parameter  $\eta$ . (3) Finally, since the radio emission flux value  $S_\nu \propto K_{\text{ep}} \nu^{-\alpha} B_d^{\alpha+1}$  is strongly dependent upon the magnetic field strength, its value  $B_d$  is derived from the fit to the *observed amplitude* of the radio spectrum. Thus, three measured characteristics of the synchrotron spectrum — X-ray flux, shape, and amplitude of the radio emission — make it possible to obtain an estimate of the three relevant “theory parameters”  $B_d$ ,  $K_{\text{ep}}$  and  $\eta$  even though this is not a simple three-step procedure but an iterative procedure, minimizing the combined  $\chi^2$ -value (see Berezhko et al. 2009, for details).

Note that the magnetic field value  $B_d$  can also be estimated by another, independent method, namely from a fit of the *observed spatial fine structure* of the X-ray emission. In all the cases where such measurements exist, both methods give consistent values of  $B_d$  (e.g., Völk et al. 2005). Unfortunately, the fine structure of the X-ray emission is not determined yet for G1.9+0.3. Therefore, this consistency check cannot be made at present.

The uncertainties of the estimated values of  $\eta$ ,  $B_d$ , and  $K_{\text{ep}}$  depend upon the quality of the measurements of the synchrotron spectrum and can be rather small, as it was recently demonstrated for the case of SN 1006 (Berezhko et al. 2009). In the case under consideration it is about 20% for  $B_d$  and  $K_{\text{ep}}$  and 30% for  $\eta$ .

It should also be noted that due to the very low age of the SNR and the low ISM density the expected thermal X-ray emission is far below the observed X-ray flux, which is therefore completely dominated by the nonthermal component.

The required proton injection rate  $\eta = 10^{-3}$  is considerably higher than the critical value  $\eta_* \approx 10^{-4}$ , which separates a nonlinearly modified shock with  $\eta > \eta_*$  from an unmodified state, resulting from very low injection rates  $\eta < \eta_*$  (see Berezhko & Ellison 1999, Eq.38). The relatively weak shock modification is the result of the very large magnetic field  $B_0$ , that leads to strong gas heating within the precursor region  $r > R_s$ .

In order to check the sensitivity of the results to the adopted value of the parameter  $\alpha_H$ , calculations with  $0.02 \leq \alpha_H < 1$  were performed. It turned out that even for  $\alpha_H = 0.02$  the shock properties are not very far from the case  $\alpha_H = 1$ : the required far upstream magnetic field value is  $B_0 = 125$   $\mu\text{G}$ , and the shock compression ratios are  $\sigma = 6.3$  and  $\sigma_s = 3.99$ .

It is noted here that the results of Vladimirov et al. (2008) suggest a stronger sensitivity of the shock properties to the value of  $\alpha_H$ . The reason is that in the considerations of these authors the parameter  $\alpha_H$  determines not only the gas heating through the term  $-\alpha_H c_A \partial P_c / \partial r$ , but also the upstream magnetic field generation through a complementary term  $(\alpha_H - 1) c_A \partial P_c / \partial r$ . Such an ap-

proach implies that magnetic field amplification takes place only due to resonant excitation of Alfvén waves and, in addition, according to such a quasi-linear expression. In contrast, the present model allows that the magnetic field is also amplified nonresonantly (Bell 2004; Pelletier et al. 2006). Secondly, the determination of the amplified field  $B_0(t_{\text{SN}})$  in the present semi-empirical model uses the synchrotron observations of the source. For both these reasons, the magnetic field amplification and the gas heating are not connected by a simple relation.

### 3.1. Subshock dynamics with amplified B-field

Following McKenzie & Völk (1982) and Vladimirov et al. (2008), an Alfvénic connection  $\mathbf{w} = \mathbf{B}(4\pi\rho)^{-1/2}$  between the magnetic field fluctuation vector  $\mathbf{B}$  and the fluctuation vector  $\mathbf{w}$  of the mass velocity is assumed. This implies an approximately incompressible plasma turbulence with a locally homogeneous mass density  $\rho$ , where the total (mean square magnetic field plus plasma turbulent) pressure is given by  $P_{\text{turb}} = (\mathbf{B})^2/(8\pi)$ , and the total (mean square magnetic field plus plasma turbulent) energy flux density equals  $F_{\text{turb}} = 3uP_{\text{turb}}$ ; here  $u$  denotes the shock-normal mean mass velocity in the shock frame. These normal components of the momentum and energy flux densities, immediately upstream and downstream of the subshock were included in the Rankine–Hugoniot conditions for the subshock. The latter is approximated as a locally plane, normal shock wave. (In the precursor region,  $(\mathbf{B})^2 = B^2$  is the mean square strength of the amplified magnetic field  $B$ , introduced in the previous section and assumed here to be isotropically distributed with Gaussian statistics; the field strength downstream of the subshock is taken to be  $B_2 = \sigma_s B_1$ , where  $B_1$  is the field strength upstream of the subshock.) Note that the above expression for the total turbulent energy flux density  $F_{\text{turb}}$  in the downstream region differs somewhat from the expression used by Caprioli et al. (2008). Since the consideration of these authors is based on the transmission and reflection of small-amplitude Alfvén waves at purely parallel subshock, it is believed here that this linear treatment is not applicable to the actual case of a strongly perturbed and amplified magnetic field (see also the arguments of Vladimirov et al. (2008)).

It is clear that the approximations introduced above do not exactly describe the true physical situation that also contains the nonresonantly unstable modes of the Bell instability (Bell 2004), because these transverse modes will in their nonlinear evolution also develop compressible elements (Bell 2004; Zirakashvili et al. 2008). In addition, also the acoustic modes (Dorfi 1984; Drury 1984; Berezhko 1986; Malkov & Diamond 2006) will contribute. Their influence on the strength of the subshock remains to be evaluated. However it is believed that the present description gives a roughly correct estimate of the subshock effects of at least the incompressible part of the fluctuation fields produced by the accelerating particles.

In the adopted approximation  $\sigma = 4.55$ ,  $\sigma_s = 3.6$  for  $\alpha_H = 1$ , very close to the previous case, where the turbulent momentum and energy fluxes were ignored in the subshock conservation relations. The effect is somewhat larger for the smallest value of the parameter  $\alpha_H = 0.02$ : it leads to a decrease of  $\sigma$  from  $\sigma = 6.3$  to  $\sigma = 5.9$

and to a decrease of the magnetic field strength from  $B_0 = 125 \mu\text{G}$  to  $B_0 = 120 \mu\text{G}$ , which is not a large effect either.

It should also be noted that the assumption of considerable gas heating due to wave dissipation, corresponding to  $\alpha_H = 0.5 - 1$ , is consistent with the numerical modeling of the nonresonant wave excitation (Bell 2004; Zirakashvili et al. 2008). Such dissipation should operate in a similar way for the resonant Alfvén mode instability. It is therefore concluded that insignificant gas heating, which occurs for  $\alpha_H \ll 1$  within the present formalism, is an unrealistic assumption.

### 3.2. Charged particle and $\gamma$ -ray spectra

With the renormalization  $f_{\text{re}} = 0.2$ , the nuclear CRs inside G1.9+0.3 SNR contain (Figure 1(c))

$$E_c \approx 0.0025 E_{\text{SN}} \approx 3 \times 10^{48} \text{ erg.} \quad (2)$$

The volume-integrated (or overall) CR spectrum

$$N(p, t) = 16\pi^2 p^2 \int_0^\infty dr r^2 f(r, p, t) \quad (3)$$

has, for the case of protons, almost a pure power-law form  $N \propto p^{-\gamma}$  over a wide momentum range from  $0.1 m_p c$  up to the cutoff momentum  $p_{\text{max}} \approx 3 \times 10^6 m_p c$  (Figure 2). This value  $p_{\text{max}} \propto R_s V_s B_0$  is limited mainly by the finite size and speed of the shock, its deceleration and the adiabatic cooling effect in the downstream region (see Berezhko 1996, for details). As pointed out above, particle diffusion is approximated by Bohm diffusion in the amplified magnetic field  $B$ , cf. Equation (1). It is important to note that the calculated value of  $p_{\text{max}}$  is therefore an upper limit, because it is assumed that up to the cutoff all particles “see” the amplified field everywhere.

Consequently, G1.9+0.3 represents the youngest SNR where the accelerated proton spectrum extends up the so-called knee energy. Such a maximum proton energy appears indeed required to describe the overall CR spectrum for energies up to  $10^{17}$  eV (Berezhko & Völk 2007).

The shape of the overall electron spectrum  $N_e(p)$  deviates from that of the proton spectrum  $N(p)$  at high momenta  $p > p_1 \sim 10^3 m_p c$  on account of the synchrotron losses during the electron residence time in the downstream region (Figure 2). Within the momentum range  $p_1 < p < p_{\text{max}}^e$ , the electron spectrum is considerably steeper,  $N_e \propto p^{-3}$ , due to synchrotron losses taking place in the downstream region after the acceleration at the shock front. The maximum electron momentum  $p_{\text{max}}^e \approx 10^5 m_p c$  corresponds closely to the result obtained by equating the synchrotron loss time and the acceleration time.

Figure 3 illustrates the consistency of the synchrotron spectrum, calculated for the above-mentioned best set of parameters with the observed spatially integrated spectra.

As mentioned above, values  $\alpha > 0.5$  of the radio spectral index  $\alpha = -d \ln S_\nu / d \ln \nu$ , as observed in young SNRs, require a curved electron spectrum that hardens toward higher energies, as predicted by nonlinear shock acceleration theory. To have  $\alpha = 0.62$  in the radio range, as observed for G1.9+0.3 (Green et al. 2008), requires efficient CR acceleration with a proton injection rate  $\eta = 10^{-3}$  which leads to the required shock modification,

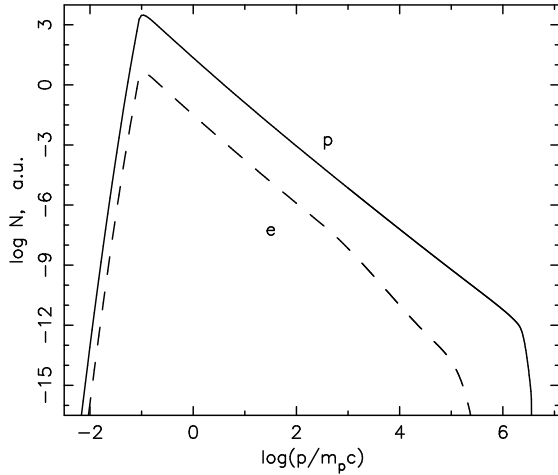


FIG. 2.— Spatially integrated CR spectrum as function of particle momentum. Solid and dashed lines correspond to protons and electrons, respectively.

and also leads to the high magnetic field value above. As it is clear from Figure 3, a good fit of the observed X-ray energy flux can only be achieved due to the softening of the synchrotron spectrum for  $\nu \gtrsim 10^{15}$  Hz, which is due to the strong synchrotron losses of electrons with momenta  $p > p_1 \approx 700 m_p c$ . Using the known dependence  $p_1 \propto B_d^{-2} t^{-1}$ , at  $t = t_{\text{SN}}$  one can immediately estimate the required value of the interior magnetic field value  $B_d \approx 500 \mu\text{G}$ , consistent with the above determination from the radio spectrum. The calculated hard power-law X-ray spectrum continues almost up to 50 keV, making this source in principle attractive to be observed with *Suzaku* and *INTEGRAL* and the future Astro-H X-ray instrument.

A very important question for every young SNR is whether the existing data indeed unavoidably require efficient proton acceleration accompanied by strong magnetic field amplification. In order to explore the alternative possibility, Figure 3 presents in the dotted curve a synchrotron spectrum which corresponds to a hypothetical leptonic scenario with a proton injection rate so small ( $\eta \ll 10^{-4}$ ) that the accelerated nuclear CRs do not produce any significant shock modification and therefore also no magnetic field amplification. This corresponds to the test particle limit, when the distribution function of shock accelerated electrons has the form

$$f_e = A p^{-4} \exp(-p/p_{\text{max}}), \quad (4)$$

where the amplitude  $A$  and the value of the cutoff momentum  $p_{\text{max}}$  are determined by the fit to the observed synchrotron spectrum for a given interior magnetic field value  $B_d$ . Since magnetic field amplification is not expected in this case, the downstream magnetic field cannot be larger than the MHD-compressed ISM field  $B_{\text{ISM}} \approx 5 \mu\text{G}$ . The maximal possible downstream field  $B_d \approx 20 \mu\text{G}$  is adopted which corresponds to the minimal number of accelerating electrons, and therefore the  $\gamma$ -ray emission produced by these electrons is also minimal. The synchrotron spectrum for the leptonic test particle scenario in Figure 3 corresponds to the maximal electron energy  $\epsilon_{\text{max}}^e = p_{\text{max}}^e c = 6 \text{ TeV}$ , determined by the *Chandra* observation. There are two differences in the synchrotron spectra, corresponding to these two scenarios. The high-injection scenario leads to a soft ra-

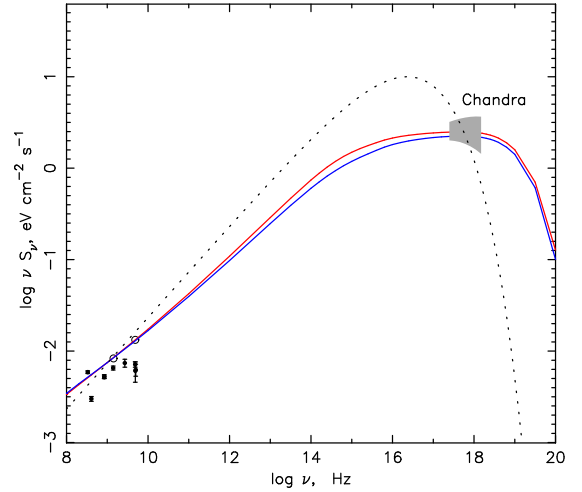


FIG. 3.— Spatially integrated synchrotron SED as a function of frequency. The dotted line corresponds to the test particle limit (leptonic scenario). Fluxes of the X-ray emission observed by *Chandra* (Reynolds et al. 2008) and the radio emission compiled by Green et al. (2008) are also shown. The solid lines are fitted to the most recent VLA radio data shown by the open circles, reported by Green et al. (2008). The line colors have the same meaning as in Figure 1.

dio spectrum  $S_\nu \propto \nu^{-\alpha}$  with power law index  $\alpha = 0.62$ , whereas in the test particle case  $\alpha = 0.5$ . On the other hand, the two spectra behave essentially differently at X-ray frequencies  $\nu \gtrsim 10^{18}$ . This demonstrates that only in the high-injection case with its high, amplified magnetic field value  $B_d \approx 460 \mu\text{G}$  the spectrum  $S_\nu(\nu)$  has a smooth cutoff, consistent with the observations (see Figure 3). In the test particle case the spectrum  $S_\nu(\nu)$  has too sharp a cutoff to be consistent with the observations.

If G1.9+0.3 was indeed a Type Ia SN, then the explosion parameters  $E_{\text{SN}}$ ,  $M_{\text{ej}}$  and  $k$  are known. Assuming the value  $d = 8.5 \text{ kpc}$  for the source distance and using the age  $t_{\text{SN}}$  and the ambient gas number density  $N_{\text{H}}$  from fits to the observed astronomical parameters size and expansion rate, and also using the “theory parameter” values  $\eta$ ,  $K_{\text{ep}}$  and  $B_0$ , estimated from the fit to the synchrotron spectrum, one can predict the  $\gamma$ -ray flux for the assumed source distance  $d$ .

In Figure 4, the calculated  $\gamma$ -ray spectral energy distributions (SEDs) due to  $\pi^0$ -decay and inverse Compton (IC) collisions are presented for the source distance  $d = 8.5 \text{ kpc}$  together with the sensitivities of the *Fermi* and H.E.S.S. instruments. For the modified shock, consistent with the observed synchrotron emission, the expected total TeV  $\gamma$ -ray SED is  $\epsilon_\gamma F_\gamma \approx 3 \times 10^{-3} \text{ eV cm}^{-2} \text{ s}^{-1}$ . Such a flux is too low for an H.E.S.S. detection in  $\sim 50 \text{ hr}$  by a factor of the order of 30. The  $\pi^0$ -decay flux is only about 6% of the IC  $\gamma$ -ray flux as a result of the low gas density. Since according to recent estimates (Porter et al. 2006), the Galactic interstellar optical and infrared radiation fields in the inner Galaxy are considerably higher than previously thought, for this region the calculation of the IC flux was performed on the basis of those estimates. The higher radiation field leads to an increase of the IC gamma-ray flux at energies  $\epsilon_\gamma < 1 \text{ TeV}$  by an order of magnitude compared with a standard interstellar radiation field in the solar neighborhood (e.g. Drury et al. 1994). Nevertheless, as indicated above, the expected TeV emission flux is still far below the H.E.S.S. sensitiv-



ity.

As can be seen from Figure 4, the TeV  $\gamma$ -ray flux expected in the unmodified leptonic scenario considerably exceeds the H.E.S.S. sensitivity, corresponding to  $\sim 50$  hr of observation time. Since the region of the Galactic center was already explored by H.E.S.S. for times of more than 100 hr without detection of G1.9+0.3, this purely leptonic test particle scenario should be rejected as in all similar cases of Type Ia SNe (Völk et al. 2008).

### 3.3. Dependence on the assumed source distance

It is, however, to be noted that the expected  $\gamma$ -ray flux is very sensitive to the assumed source distance  $d$ . Therefore, SNR G1.9+0.3 could be a potential  $\gamma$ -ray source if the actual distance was lower than 8.5 kpc. Qualitatively, the dependence of the expected  $\gamma$ -ray flux on distance can be understood if one takes into account that the  $\pi^0$ -decay  $\gamma$ -ray energy flux  $\epsilon_\gamma F_\gamma \propto M_{\text{sw}} e_c / d^2$  is proportional to the mass of gas,  $M_{\text{sw}} = 4\pi R_s^3 \rho_0 / 3$ , swept up by the SN shock, and to the energy density  $e_c$  of the CRs producing  $\gamma$ -rays of given energy. Since for high acceleration efficiency  $e_c$  is proportional to the shock kinetic energy density  $\rho_0 V_s^2$ , one can write

$$\epsilon_\gamma F_\gamma \propto N_H^2 V_s^2 R_s^3 / d^2. \quad (5)$$

For fixed explosion energy  $E_{\text{SN}}$ , the distance  $d$  and ISM density  $N_H$  are connected by the relation

$$N_H \propto d^{-7}, \quad (6)$$

because in the free expansion phase the SNR radius  $R_s \propto d$  is determined by the expression  $R_s \propto N_H^{-1/7} t^{4/7}$  (Chevalier 1982), where the SNR age  $t \propto R_s / V_s$  is fixed if the angular size and angular expansion speed are known as in our case of G1.9+0.3.

Taking also into account that for a fixed angular expansion rate of the object  $V_s \propto d$ , one obtains

$$\epsilon_\gamma F_\gamma \propto d^{-11}. \quad (7)$$

According to this relation a mere 30% reduction of the source distance leads to an increase of the expected  $\gamma$ -ray flux by a factor of more than 10. This is illustrated in Figure 4, where also  $\gamma$ -ray spectra are presented that were calculated for the distance value  $d = 5.6$  kpc. In this case the shock velocity and size could be fitted at the same age  $t_{\text{SN}} = 80$  yr and for an ISM hydrogen number density  $N_H = 0.2 \text{ cm}^{-3}$ . A similar fit for the radio and X-ray data as in Figure 4 could be achieved with an electron-proton ratio  $K_{\text{ep}} = 8 \times 10^{-4}$  and a downstream magnetic field strength  $B_d = 670 \mu\text{G}$ . It is clear that G1.9+0.3 could be visible in TeV  $\gamma$ -rays by future instruments like the Cherenkov Telescope Array (CTA), if the actual distance was not larger than  $d = 5.6$  kpc.

The theoretical, spatially integrated radio synchrotron flux slowly increases with time, as can be seen in Figure 5, essentially due to the rapidly increasing total number of accelerated electrons in the increasing SNR volume  $\propto R_s^3$ .

The X-ray synchrotron flux is expected to be nearly constant in time (Figure 5). This is mainly due to the strong synchrotron cooling of the highest energy electrons which produce the X-ray synchrotron emission.

The TeV  $\gamma$ -ray flux is expected to increase with time as well (Figure 5), mainly due to the increase of overall number of CRs with energy above 10 TeV.

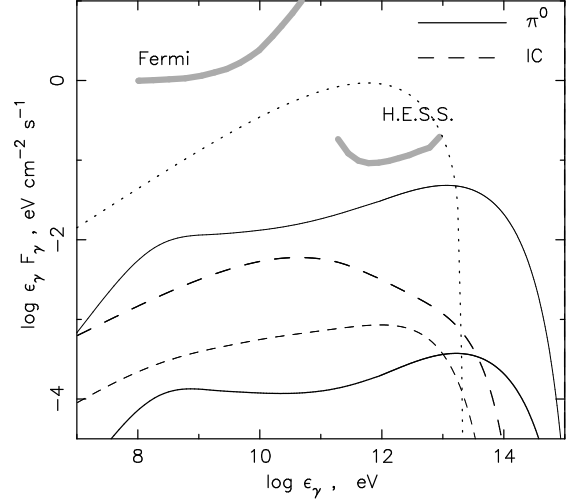


FIG. 4.— Integral  $\pi^0$ -decay (solid lines) and IC (dashed lines)  $\gamma$ -ray energy flux densities (SEDs) for the present epoch, as a function of  $\gamma$ -ray energy, for the two different source distances  $d = 8.5$  kpc (thick lines) and  $d = 5.6$  kpc (thin lines). The calculations are given for the case  $\delta = 1$ . SEDs calculated for the case  $\delta = 3/2$  coincide with the presented SEDs within 10% accuracy. The thick dashed line represents the IC  $\gamma$ -ray energy flux, calculated for the recently re-estimated interstellar optical/infrared radiation background in the central region of the Galaxy (Porter et al. 2006). The dotted line corresponds to the test particle limit (leptonic scenario). For comparison, the sensitivities of *Fermi* (for a  $5\sigma$  detection in 1 yr of sky survey exposure with a background representative of the diffuse background near the galactic plane; Atwood et al. (2009)) and H.E.S.S. (for a  $5\sigma$  detection of the Crab Nebula with power-law differential photon index 2.6 in 50 hr at a zenith angle of  $20^\circ$ ; Funk (2005)) are shown.

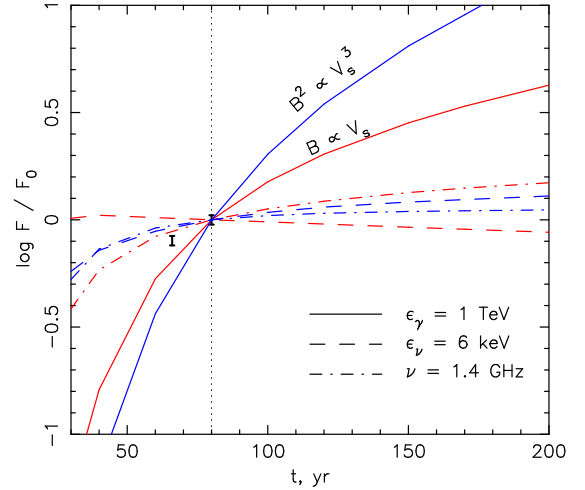


FIG. 5.— Time dependence (in years) of the fluxes of the radio synchrotron emission at frequency  $\nu = 1.4$  GHz (dash-dotted lines), synchrotron X-ray emission with energy  $\epsilon_\nu = 6$  keV (dashed lines), and TeV energy  $\gamma$ -ray emission (solid lines). The fluxes are normalized to their values  $F_0$  at the current epoch. Available data in radio (Green et al. 2008) are shown as well. The line colors have the same meaning as in Figure 1.

### 3.4. Renormalization of the nuclear particle spectra

If the ambient interstellar magnetic field would be completely disordered on spatial scales smaller than the shock size, then efficient CR injection/acceleration would be expected across the whole shock surface. In such a case  $f_{\text{re}} \approx 1$  and the expected gamma-ray flux would be higher by a factor of  $1/f_{\text{re}} \approx 5$ , whereas all the emission produced by CR electrons would remain the

same since the normalization of the electron spectrum was done based on the observations. However, it is believed that the actual situation is opposite: the bilateral symmetry of the X-ray synchrotron emission suggests a roughly uniform ambient magnetic field on a parsec scale and therefore  $f_{\text{re}} \approx 0.2$  like in SN 1006.

#### 4. CONCLUSIONS

The existing data for G1.9+0.3, when analyzed within the framework of the nonlinear kinetic theory of CR production in SNRs described above, are consistent with a type Ia explosion in a rarefied medium at a distance of  $d = 8.5$  kpc, whose nuclear CR spectrum reaches the energy of the “knee” in the observed Galactic CR spectrum at the present epoch. This conclusion also concerns the derived strong magnetic field amplification. A test particle, purely leptonic gamma-ray scenario, is inconsistent with existing TeV gamma-ray observations with the H.E.S.S. telescope array. However, the data set is not complete enough to unequivocally determine the value of the source distance. Since the expected  $\gamma$ -ray flux is very sensitive to the distance  $d$ ,  $F_\gamma \propto d^{-11}$ , a detec-

tion of the  $\gamma$ -ray flux from G1.9+0.3, as improbable as it may be, would yield the distance. However, in the case when G1.9+0.3 is located near the Galactic center ( $d = 8.5$  kpc), the expected TeV  $\gamma$ -ray energy flux is so low,  $\epsilon_\gamma F_\gamma \approx 5 \times 10^{-15}$  erg cm $^{-2}$  s $^{-1}$ , that it is not detectable with present instruments. It is clear that for a distance that was not larger than  $d = 5.6$  kpc G1.9+0.3 could be visible with future instruments like CTA which can be assumed to have a sensitivity of  $\sim 1$  mcrab at a few 100 GeV (Bernlöhr 2009).

We are indebted to Dr. Stephen Reynolds for providing us the X-ray spectra for G1.9+0.3 from *Chandra* in physical units. This work has been supported in part by the Russian Foundation for Basic Research (grants 07-02-00221, 10-02-00154), Federal Agency of Science and Innovations (contract 02.740.11.0248), Program of PRAS No. 16 and by the Leading Scientific Schools of Russia (project 3526.2010.2). EGB and LTK acknowledge the hospitality of the Max-Planck-Institut für Kernphysik, where part of this work was carried out.

#### REFERENCES

- Aharonian, F., et al. 2006, *ApJ*, 636, 777  
 Atwood, W.B., et al. 2009, *ApJ*, 697, 1071  
 Bell, A.R. 2004, *MNRAS*, 353, 550  
 Bell, A.R. & Lucek, S.G. 2001, *MNRAS*, 321, 433  
 Berezhko, E.G. 1986, *Sov. Astron. Lett.*, 12, 352  
 Berezhko, E.G. 1996, *Astropart. Phys.*, 5, 367  
 Berezhko, E.G. 2005, *Adv. Space Res.*, 35, 1031  
 Berezhko, E.G. 2008, *Adv. Space Res.*, 41, 429  
 Berezhko, E.G., & Ellison, D.C. 1999, *ApJ*, 526, 385  
 Berezhko, E.G., Elshin, V.K., & Ksenofontov, L.T. 1996, *J. Exp. Theor. Phys.*, 82, 1  
 Berezhko, E.G., Ksenofontov, L.T., & Völk, H.J., 2009, *A&A*, 505, 169  
 Berezhko, E.G., & Völk, H.J. 1997, *Astropart. Phys.*, 7, 183  
 Berezhko, E.G., & Völk, H.J. 2007, *ApJ*, 661, L175  
 Bernlöhr, K. 2009, in *AIP Conf. Proc.* 1085, *High Energy Gamma-Ray Astronomy*, ed. F.A. Aharonian, W. Hofmann, & F.M. Rieger, (Melville, NY: AIP), 874  
 Caprioli, D., Blasi, P., Amato, E., & Vietri, M. 2008, *ApJ*, 679, L139  
 Chevalier, R.A. 1982, *ApJ*, 258, 790  
 Dorfi, E.A., 1984, *Adv. Space Res.*, 4, 205  
 Drury, L.O’C., 1984, *Adv. Space Res.*, 4, 191  
 Drury, L.O’C., Aharonian, F.A. & Völk, H.J., 1994, *A&A*, 287, 959  
 Funk, S. 2005, PhD thesis, Univ. Heidelberg, Germany  
 Green, D.A., & Gull, S.F. 1984, *Nature*, 312, 527  
 Green, D.A., et al. 2008, *MNRAS*, 387, L54  
 Kang, H., & Jones, T.W. 2006, *Astropart. Phys.*, 25, 246  
 Lucek, S.G. & Bell, A.R. 2000, *MNRAS*, 314, 65  
 Malkov, M.A., & Diamond, P.H. 2006, *ApJ*, 642, 244  
 McKenzie, J.F., & Völk, H.J. 1982, *A&A*, 116, 191  
 Murphy, T., Gaensler, B.M., & Chatterjee, S. 2008, *MNRAS*, 389, L23  
 Niemiec, J., Pohl, M., Stroman, T. & Nishikawa, K. 2008, *ApJ*, 684, 1174  
 Ohira, Y., Reville, B., Kirk, J.G., & Takahara, F. 2009, *ApJ*, 698, 445  
 Pelletier, G., Lemoine, M., & Marcowith, A. 2006, *A&A*, 453, 181  
 Porter, T.A., Moskalenko, I.V., & Strong, A.W. 2006, *ApJ*, 648, L29  
 Reville, B., O’Sullivan, S., Duffy, P., & Kirk, J.G. 2008, *MNRAS*, 386, 509  
 Reynolds, S.P., et al. 2008, *ApJ*, 680, L41  
 Reynolds, S.P., et al. 2009, *ApJ*, 695, L149  
 Riquelme, M.A., & Spitkovsky, A. 2009, *ApJ*, 649, 626  
 Vladimirov, A.E., Bykov, A.M., & Ellison, D.C. 2008, *ApJ*, 688, 1084  
 Völk, H.J. 2004, in *Proc. 28th Int. Cosmic Ray Conf.* (Tsukuba) 8, *Frontiers of Cosmic Ray Science*, ed. T. Kajita, et al. (Tokyo, Japan, Universal Academy Press), 29  
 Völk, H.J., Berezhko, E.G., & Ksenofontov, L.T. 2003, *A&A*, 409, 563  
 Völk, H.J., Berezhko, E.G., & Ksenofontov, L.T. 2005, *A&A*, 433, 229  
 Völk, H.J., Berezhko, E.G., & Ksenofontov, L.T. 2008, *A&A*, 490, 515  
 Zirakashvili, V.N. & Ptuskin, V.S. 2009, in *AIP Conf. Proc.* 1085, *High Energy Gamma-Ray Astronomy*, ed F.A. Aharonian, W. Hofmann, & F.M. Rieger, (Melville, NY: AIP), 336  
 Zirakashvili, V.N., Ptuskin, V.S., & Völk, H.J., 2008, *ApJ*, 678, 255